ON THE THEORY OF TWO-PHOTON INTERSUBBAND ABSORPTION AND LINEAR-CIRCULAR DICHROISM IN SEMICONDUCTORS OF THE A₃B₅ TYPE

ⓘRustam Y. Rasulov[a], ⓘVokhob R. Rasulov[a]*, Forrukh U. Kasimov[b], Mardonbek Kh. Nasirov[a,c],
Islam E. Farmanov[a], Abay Z. Tursinbaev[d]

a Fergana State University, Fergana, Uzbekistan
b Andijan State University, Andijan, Uzbekistan
c Fergana State Technical University, Fergana, Uzbekistan
d South Kazakhstan University of Muktar Auezov, Shymkent, Kazakhstan
Corresponding Author e-mail: vrrasulov83@gmail.com
Received August 6, 2024; revised April 13, 2025; accepted April 23, 2025

The frequency-temperature dependences of the probability of two-photon absorption (2PA), caused by transitions from the branch of light holes to the subband of spin-orbit splitting and linear-circular dichroism (LCD) associated with 2PA, as well as the coefficient of two-photon light absorption in *GaAs* and InAs, where the contribution to the absorption of the effect of coherent saturation. The role of various types of transitions, differing from each other in virtual states and participating in the 2PT, is analyzed. In *GaAs* and *InAs*, the presence of several peaks in the frequency-temperature dependences of the 2PA coefficient was revealed; the appearance of the peaks is explained not only by a specific change in the distribution functions of photoexcited holes, but also by the fact that at certain frequency values, some denominators in the expressions of the composite matrix elements tend to zero.

Keywords: *Two-photon optical transitions; Virtual states; Multiphoton optical transitions; Two-photon absorption coefficient; Coherent saturation effect; Semiconductor*
PACS: 71.20. – b, 71.28. + d

INTRODUCTION

Nonlinear spectroscopy of solids has proven invaluable in determining their optical and electronic parameters. For instance, when single-photon absorption is forbidden by selection rules, multiphoton transitions may become allowed [1]. The processes of multiphoton absorption in crystals have been the subject of extensive theoretical and experimental studies since the advent of the laser (see, for example, [2–7]). This interest in multiphoton absorption has been driven by the significance of nonlinear absorption facilitated by powerful lasers and masers, as well as its role in numerous aspects of fundamental research in semiconductor physics. It should be noted that in the processes of electron-hole pair generation induced by intense optical radiation, both in bulk [2–13] and low-dimensional crystals, multiphoton interband and intraband transitions play a critical role [14–24].

Although [14–24] investigated optical phenomena in bulk and low-dimensional crystals, where either interband transitions or transitions between the branches of light and heavy holes are restricted, the question of single- and multiphoton absorption of linearly and circularly polarized light in narrow- and wide-bandgap semiconductors, driven by optical transitions from the branches of light and heavy holes to the spin-orbit split subband of the valence band, remains unresolved. This study is dedicated to addressing this issue.

Effective Luttinger–Kohn Hamiltonian for III–V Semiconductors (GaAs, InAs) Formulation of the Luttinger–Kohn Hamiltonian

In zincblende III–V semiconductors, the top valence bands (heavy-hole, light-hole, and split-off bands) are described by the Luttinger–Kohn (LK) Hamiltonian derived from $k \cdot p$ theory. This effective Hamiltonian acts on the Bloch states at the Brillouin-zone center with total angular momentum $j = 3/2$ (degenerate heavy-hole and light-hole, Γ_8 symmetry) and $j = 1/2$ (split-off band, Γ_7) due to the spin–orbit interaction. The LK Hamiltonian is a 6×6 matrix (or 4×4 if the split-off band is excluded) built from the angular momentum $J = 3/2$ matrices $\hat{J}_x, \hat{J}_y, \hat{J}_z$ and wavevector components k_x, k_y, k_z. To second order in **k**, the general form can be written (in the $j = 3/2$ basis) as a quadratic form in $k_i k_j J_i J_j$ terms with three dimensionless Luttinger parameters $\gamma_1, \gamma_2, \gamma_3$. In an isotropic approximation (neglecting cubic anisotropy), the Hamiltonian simplifies to:

$$H_{LK} = \frac{\hbar^2}{2m_0}\left[\left(\gamma_1 + \frac{5}{2}\gamma_2\right)k^2 - 2\gamma_2(\boldsymbol{k} \cdot \boldsymbol{J})^2\right],$$

where m_0 is the free electron mass, $k^2 = k_x^2 + k_y^2 + k_z^2$, and $\mathbf{k} \cdot \mathbf{J} = k_x\hat{J}_x + k_y\hat{J}_y + k_z\hat{J}_z$. This is the so-called spherical approximation ($\gamma_2 = \gamma_3$), which is often used for simplicity. In the general case for cubic crystals, $\gamma_2 \neq \gamma_3$, and one must

include distinct terms for $\hat{J}_i^2 k_i^2$ and the off-diagonal couplings $\hat{J}_i, \hat{J}_j k_i, k_j$ (which cause band warping). An explicit representation of the full 4×4 LK Hamiltonian (for the $j = 3/2$ subspace) in the Bloch basis $|3/2, m_j\rangle$ is

$$H_{LK}^{4\times4} = \frac{\hbar^2}{2m_0} \begin{pmatrix} A & -B & C & 0 \\ -B^* & D & 0 & C \\ C^* & 0 & D & B \\ 0 & C^* & B^* & A \end{pmatrix}$$

where (suppressing factor $\hbar^2/2m_0$) $A = \gamma_1 k^2 + (\gamma_2 + \gamma_3)(k_x^2 + k_y^2 - 2k_z^2)$, $D = \gamma_1 k^2 + (\gamma_2 + \gamma_3)(k_z^2 + k_y^2 - 2k_x^2)$ (cyclic permutations for D) and the off-diagonal couplings are $B = 2\sqrt{3}, \gamma_3, k_z(k_x - ik_y)$, $C = -\sqrt{3}, \gamma_2, (k_x^2 - k_y^2) + 2i\sqrt{3}, \gamma_3, k_x k_y$. (Here the basis is ordered as $|3/2, +3/2\rangle, |3/2, -1/2\rangle, |3/2, +1/2\rangle, |3/2, -3/2\rangle$ for this matrix.) The 6×6 Hamiltonian including the split-off $j = 1/2$ states is an extension of the above, with the spin–orbit energy Δ_{SO} separating the Γ_7 band on the diagonal and additional k-dependent coupling terms between $j = 3/2$ and $j = 1/2$ blocks. In the absence of inversion asymmetry (no bulk inversion asymmetry term $B = 0$ for centrosymmetric zincblende), the above H_{LK} is the standard effective Hamiltonian for holes in III–V compounds first formulated by Luttinger (1956). Eigenenergies and Eigenfunctions Zone-center basis: At $k = 0$ (the Γ point), the valence-band edges consist of a four-fold degenerate Γ_8 state (spin–orbit j=3/2 quartet) and a split-off Γ_7 doublet separated by Δ_{SO}. One convenient choice of orthonormal Bloch basis for the Γ_8 valence states is in terms of spin–orbit coupled atomic p-orbitals $|X\rangle, |Y\rangle, |Z\rangle$ and spin $\uparrow, \downarrow$. For example:

$$|3/2, +3/2\rangle = \frac{-1}{\sqrt{2}}(|X + iY\rangle \uparrow),$$

$$|3/2, +1/2\rangle = \frac{-1}{\sqrt{6}}(|X + iY\rangle \downarrow) + \sqrt{\frac{2}{3}}(|Z\rangle \uparrow,$$

$$|3/2, -1/2\rangle = \frac{1}{\sqrt{6}}(|X - iY\rangle \uparrow) + \sqrt{\frac{2}{3}}(|Z\rangle \downarrow),$$

$$|3/2, -3/2\rangle = \frac{1}{\sqrt{2}}(|X - iY\rangle \downarrow),$$

up to overall phase factors. Here $|3/2, \pm3/2\rangle$ are "heavy-hole" (HH) states with angular momentum projection $m_j = \pm3/2$ (maximally aligned orbital and spin), and $|3/2, \pm1/2 >$ are "light-hole" (LH) states ($m_j = \pm1/2$) which are a mixture of spin-up and spin-down with the p_z-orbital character. The split-off $|1/2, \pm1/2\rangle$ states (not written above) are primarily p_z-type with opposite spin mixture and lie Δ_{SO} lower in energy.

Dispersion and effective masses: For a given wavevector **k**, one finds the band energies by diagonalizing H_{LK}. Along high-symmetry axes, the eigenstates can often be chosen as pure m_j states. For example, if **k** is taken along the z-axis ([001] direction), then $\hat{J}z$ commutes with HLK, so m_j remains a good quantum number. In this case, the HH states ($m_j = \pm3/2$) decouple from the LH states ($m_j = \pm1/2$), yielding parabolic dispersions:

Heavy-hole band: $E_{hh}(k_\parallel) = \frac{\hbar^2 k_\parallel^2}{2m_0}(\gamma_1 - 2\gamma_2)$ for $\mathbf{k} = k_\parallel \hat{z}$. This implies an effective mass $m_{hh}^{[001]} = \frac{m_0}{\gamma_1 - 2\gamma_2}$ along [001].

Light-hole band: $E_{lh}(k_\parallel) = \frac{\hbar^2 k_\parallel^2}{2m_0}(\gamma_1 + 2\gamma_2)$ for $\mathbf{k} = k_\parallel \hat{z}$, with effective mass $m_{lh}^{[001]} = \frac{m_0}{\gamma_1 + 2\gamma_2}$.

Twofold spin degeneracy is retained (e.g. $m_j = +3/2$ and $-3/2$ give the same E_{hh}). Because $\gamma_1 > \gamma_2$ for typical III–Vs, the HH band is "heavier" (larger effective mass, smaller curvature) than the LH band. For directions other than [001], the angular momentum projection is not a conserved quantum number, and the HH–LH states mix under the influence of the γ_3 terms in the Hamiltonian. This mixing leads to anisotropic dispersion or warping. For instance, for motion along the [111] direction one finds $E_{hh}(k_{[111]}) \propto (\gamma_1 - 2\gamma_3)k^2$ and $E_{lh}(k_{[111]}) \propto (\gamma_1 + 2\gamma_3)k^2$, which differ from the [001] masses if $\gamma_3 \neq \gamma_2$. In GaAs and InAs, $\gamma_3 > \gamma_2$ (see values below), so the constant-energy surfaces of the HH band are non-spherical, with the dispersion being flatter (heavier mass) along [111] than along [001]. The LK model thus captures the cubic anisotropy of the valence band, while still providing analytic eigenfunctions (four-component spinors) that are combinations of the Bloch basis states above. These LK eigenstates are used as envelope functions in envelope-function approximations for heterostructures and to calculate transition matrix elements for optical processes.

Standard Luttinger Parameters for GaAs and InAs

The Luttinger parameters ($\gamma_1, \gamma_2, \gamma_3$) are typically determined by fitting the model to experimentally measured band dispersions (effective masses) or derived from ab initio band structure calculations. Below we list representative room-temperature values for GaAs and InAs:

GaAs: $\gamma_1 \approx 6.98, \gamma_2 \approx 2.06, \gamma_3 \approx 2.93$; these differences are minor and reflect fit updates. $\Delta_{SO} \approx 0.341$ eV for GaAs.

InAs: $\gamma_1 \approx 20.0, \gamma_2 \approx 8.5, \gamma_3 \approx 9.2$ with $\Delta_{SO} \approx 0.39$ eV. These large parameter values indicate the strongly nonparabolic, highly anisotropic valence band in InAs (heavy holes in InAs have an especially large effective mass due to $\gamma_1 - 2\gamma_2$ being small).

Two-photon light absorption in A_3B_5 semiconductors

The two-photon absorption (2PA) coefficient is expressed in the following form [9–11]:

where: $f_{lh,\vec{k}}^{(2)}\left(f_{hh,\vec{k}}^{(2)}\right)$- is the distribution function of light (lh) and heavy (hh) holes, $M_{lh,m;hh,m'}^{(2)}(\vec{k})$ - is the matrix element (ME) of the transition $|hh,m\rangle \xrightarrow{2PA} |lh,m'\rangle$, $I(\omega)$- represents the intensity (or frequency, ω\omega) of light, the wave vector of holes participating in optical transitions $|hh,\pm3/2\rangle \xrightarrow{2PA} |lh,\pm1/2\rangle$, with the energy dispersion $E_{V_l}(\vec{k}) = (A - (-1)^l B)k^2 = \frac{\hbar^2}{2m_l}k^2$ ($l = 1,2$, $l = 1(hh)$, is given as:

$l = 2(lh)$-for heavy holes, the wave vector is expressed as: $k_{lh,hh}^{(2\omega)} = \left(2\mu_{lh,hh}\hbar^{-2}2\hbar\omega\right)^{1/2}$, where $\mu_{lh,hh} = \frac{m_{hh}m_{lh}}{m_{hh}-m_{lh}}$is the reduced mass of the holes.

The energy of heavy holes with such a wave vector is equal to $E_{hh}\left(k_{lh,hh}^{(2\omega)}\right) = \frac{m_{lh}}{m_{hh}-m_{lh}}2\hbar\omega$, while the energy of light holes is $E_{lh}\left(k_{lh,hh}^{(2\omega)}\right) = \frac{m_{hh}}{m_{hh}-m_{lh}}2\hbar\omega$, and their distribution functions are determined respectively as:

$$f\left[E_{hh}\left(k_{lh,hh}^{(2\omega)}\right)\right] = exp\left(-\frac{2\hbar\omega}{k_BT}\frac{m_{lh}}{m_{hh}-m_{lh}}\right) exp\left(\frac{E_F}{k_BT}\right) \tag{2}$$

and

$$f\left[E_{lh}\left(k_{lh,hh}^{(2\omega)}\right)\right] = exp\left(-\frac{2\hbar\omega}{k_BT}\frac{m_{hh}}{m_{hh}-m_{lh}}\right) exp\left(\frac{E_F}{k_BT}\right). \tag{3}$$

Calculations show that if the temperature dependence of the bandgap width, the effective masses of charge carriers, and the effect of coherent saturation are not taken into account, the distribution functions increase with temperature at a fixed frequency, reach a maximum, and then decrease. At a fixed temperature, the distribution functions decrease with increasing frequency. This behavior of the distribution functions plays a key role in the frequency-temperature dependence of the 2PA coefficient.

Further, it should be noted that in subsequent calculations, unlike in [25], it is assumed that during multiphoton transitions, virtual states exist not only in the branches of heavy and light holes but also in the spin-orbit split subband.

Quantitative calculations show that the optical transitions considered in [25] for wide-bandgap semiconductors provide the main contribution to absorption in the low-frequency region, while the contribution in the high-frequency region $\left(\Delta_{SO} \leq 2\hbar\omega \leq E_g\right)$ is less than 5%. Therefore, further analysis will focus on transitions between the light hole subband and the spin-orbit split subband, as these transitions make a significant contribution in the frequency region $\Delta_{SO} \leq 2\hbar\omega \leq E_g$ $\left(\Delta_{SO}, E_g \leq 2\hbar\omega\right)$ for wide-bandgap (narrow-bandgap) semiconductors.

Matrix elements of two-photon transitions from the light hole branch to the spin-orbit split subband

When the photon energy satisfies the condition $\Delta_{SO} \leq 2\hbar\omega$, optical transitions occur from the heavy and light hole branches to the spin-orbit split subband. In particular, two-photon optical transitions from the light hole branch of the valence band to the spin-orbit split subband occur in two stages: in the first stage, i.e., during a transition of type $|lh,\pm1/2\rangle \Rightarrow |SO,\pm1/2\rangle$, the spin direction does not change during the optical transition, while in the second stage, $|lh,\pm1/2\rangle \Rightarrow |SO,\mp1/2\rangle$ (see Fig. 1), the spin direction reverses (see Table 1).

Table 1. Composite matrix elements of optical transitions from the light and heavy hole branches to the spin-orbit split subband (each multiplied by $\left(\frac{eA_0}{(c\hbar)}\right)^2$, $e'_{\pm} = e'_x \pm ie'_y$ $e'^2_{\perp} = e'^2_x + e'^2_y$).

Virtual state	Composite matrix elements of optical transitions	
	Type 1 optical transitions (spin direction does not change)	Type 2 optical transitions (spin direction reverses)
In the branches of the valence band	$\frac{B^2k^2}{\hbar\omega\sqrt{2}}\left[\frac{3\hbar\omega}{E_{hh}-E_{lh}-\hbar\omega}e'^2_{\perp} + 4\left(\frac{A}{B}+1\right)e'^2_z\right]$	$\frac{i}{\sqrt{6}}\frac{2(A+B)P_ck}{\hbar\omega}e'_+e'_z$
In the spin-orbit split subband	$-\frac{P_c^2}{3\sqrt{2}}\frac{1}{E_{cond}-E_{lh}-\hbar\omega}\left(e'^2_{\perp}+4e'^2_z\right)$	$\frac{1}{\sqrt{2}}\frac{P_c^2}{(E_{cond}-E_{lh}-\hbar\omega)}e'_+e'_z$
In the conduction band	$2\sqrt{2}\frac{A}{B}\frac{B^2k^2}{(E_{SO}-E_{lh}-\hbar\omega)}e'^2_z$	$\frac{3\sqrt{2}ABk^2}{E_{SO}-E_{lh}-\hbar\omega}e'_ze'_+$

In Table 1: A, B -band parameters of the semiconductor, $B = \frac{\hbar^2}{4} \frac{m_{hh} - m_{lh}}{m_{lh} m_{hh}}$, bandgap parameters, P_c- Kane parameter [26, 27], $e'_\alpha (\alpha = x, y, z)$-components of the light polarization vector, A_0-amplitude of the electromagnetic wave vector potential.

In particular, for the optical transitions $|lh, \pm 1/2\rangle \xrightarrow{2PA} |SO, \pm 1/2\rangle$ shown in Fig. 1, the square of the modulus of the sum of the matrix elements (ME) is written as:

$$\left| M_{lh, \pm 1/2; SO, \pm 1/2} \right|^2 = \frac{1}{2} \left(\frac{e A_0}{c \hbar} \right)^4 \left(\frac{B^2 k^2}{\hbar \omega} \right)^2 \left(\Re_Z e'^4_z + \Re_\perp e'^4_\perp + \Re_{Z\perp} e'^2_\perp e'^2_z \right), \tag{4}$$

and for optical transitions of type $|lh, \pm 1/2\rangle \xrightarrow{2PA} |SO, \mp 1/2\rangle$:

$$\left| M_{lh, \pm 1/2; SO, \mp 1/2} \right|^2 = \left(\frac{e A_0}{c \hbar} \right)^4 \left(\frac{B k^2}{\hbar \omega} \right)^2 \Re'_{z\perp} e'^2_\perp e'^2_z, \tag{5}$$

where:

$$\Re_Z = 16 \left[\left(\frac{A}{B} \frac{\hbar \omega}{E_{SO} - E_{lh} - \hbar \omega} \right)^2 + \left(\frac{A}{B} + 1 \right)^2 + \left(\frac{P_c^2}{3B^2 k^2} \frac{\hbar \omega}{E_{cond} - E_{lh} - \hbar \omega} \right)^2 \right], \tag{6 a}$$

$$\Re_\perp = \left[\left(\frac{P_c^2}{3B^2 k^2} \frac{\hbar \omega}{E_{cond} - E_{lh} - \hbar \omega} \right)^2 + \left(\frac{3 \hbar \omega}{E_{hh} - E_{lh} - \hbar \omega} \right)^2 \right], \tag{6 b}$$

$$\Re_{Z\perp} = \left[8 \left(\frac{P_c^2}{3B^2 k^2} \frac{\hbar \omega}{E_{cond} - E_{lh} - \hbar \omega} \right)^2 + \frac{24 \hbar \omega}{E_{hh} - E_{lh} - \hbar \omega} \left(\frac{A}{B} + 1 \right) \right], \tag{6 c}$$

$$\Re'_{z\perp} = \left[\frac{4}{6} \left(\frac{A}{B} + 1 \right)^2 \left(\frac{P_c}{Bk} \right)^2 + \frac{1}{2} \left(\frac{P_c^2 \hbar \omega}{Bk^2 (E_{cond} - E_{lh} - \hbar \omega)} \right)^2 + 18 \left(\frac{A}{B} \right)^2 \left(\frac{\hbar \omega}{E_{SO} - E_{lh} - \hbar \omega} \right)^2 \right]. \tag{6 d}$$

| $|V, \pm 1/2\rangle$ ·····●·····●····· $|SO, \pm 1/2\rangle$ $|lh, m = \pm 1/2\rangle$ | $|V, \pm 1/2\rangle$ ·····●·····●····· $|SO, \pm 1/2\rangle$ $|SO, m = \pm 1/2\rangle$ | $|V, \pm 1/2\rangle$ ·····●·····●····· $|SO, \pm 1/2\rangle$ $|c, m = \pm 1/2\rangle$ | $|V, \pm 1/2\rangle$ ·····●·····●····· $|SO, \pm 1/2\rangle$ $|hh, m = \pm 3/2\rangle$ |

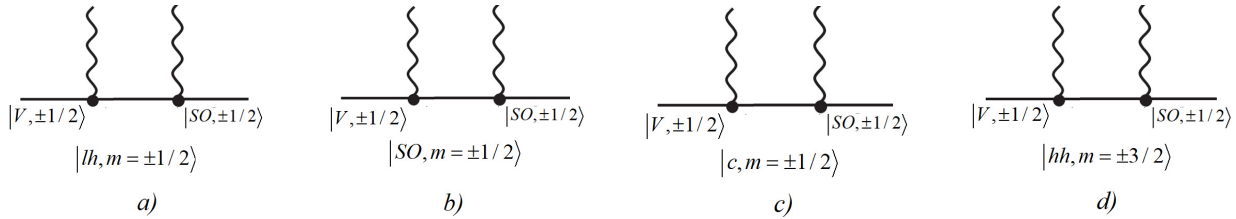*a)*   *b)*   *c)*   *d)*

Figure 1. Types of two-photon transitions from the light hole branch of the valence band to the spin-orbit split subband $|V, \pm 1/2\rangle \xrightarrow{2PA} |SO, \pm 1/2\rangle$: a) Intermediate states are located in the light hole branch; b) In the spin-orbit split subband; c) In the heavy hole subband; d) In the heavy hole subband. In such optical transitions, the spin direction of charge carriers does not change. Optical transitions involving spin flip are determined in a similar manner, where the substitution $|SO, \pm 1/2\rangle \leftrightarrow |SO, \mp 1/2\rangle$ must be applied.

It should be noted that if the energy conservation law associated with TPA is taken into account, the energies of the holes involved in optical transitions from the light hole branch to the spin-orbit split subband are determined by the following expression

$$E_c \left(k_{SO, lh}^{(2\omega)} \right) = \frac{m_{SO} \cdot m_{lh}}{m_{cond} (m_{SO} - m_{lh})} (2 \hbar \omega - \Delta_{SO}) + E_g, \tag{7}$$

$$E_{lh} \left(k_{SO, lh}^{(2\omega)} \right) = \frac{m_c}{m_c - m_{lh}} (2 \hbar \omega - \Delta_{SO}), \quad E_{hh} \left(k_{SO, lh}^{(2\omega)} \right) = \frac{m_{SO} \cdot m_{lh}}{m_{hh} (m_{SO} - m_{lh})} (2 \hbar \omega - \Delta_{SO}),$$

and their wave vector is given by: $k_{SO, lh}^{(2\omega)} = \sqrt{\frac{2 \mu_-^{(SO, lh)}}{\hbar^2} (2 \hbar \omega - \Delta_{SO})}$ where: $\mu_-^{(SO, lh)} = \frac{m_{SO} m_{lh}}{m_{SO} - m_{lh}}$ is the reduced mass of the holes, E_g (Δ_{SO})- is the bandgap width (spin-orbit splitting), m_{SO} - is the effective mass of the holes, $E_{SO}(\vec{k}) = \Delta_{SO} + \frac{\hbar^2}{2 m_{SO}} k^2$- is the energy spectrum of the holes in the spin-orbit split subband.

It should be noted that we will conventionally classify semiconductors as wide-bandgap $(E_g \rangle \Delta_{SO})$, intermediate-bandgap $(E_g \approx \Delta_{SO})$, and narrow-bandgap $(E_g \langle \Delta_{SO})$. Now, let us analyze both interband and intraband optical transitions in these semiconductors. It is known that an optical transition between the conduction band and the valence band (interband optical transition) occurs when the condition $E_g \langle 2 \hbar \omega$ is satisfied, while transitions from the light and heavy hole branches to the spin-orbit split subband (intraband optical transition) occur under the condition $\Delta_{SO} \langle 2 \hbar \omega$. Thus, the order of interband and intraband optical transitions depends on the ratio $\frac{E_g}{\Delta_{SO}}$. From this, it can be seen that as the frequency increases in wide-bandgap (narrow-bandgap) semiconductors, intraband (interband) optical transitions occur first, followed by interband (intraband) optical transitions. In intermediate-bandgap semiconductors, both interband and intraband optical transitions occur (almost) simultaneously. This implies that when studying optical transitions, special

attention must be paid to the band structure of the semiconductor, which will be taken into account in subsequent calculations and in the analysis of results.

Since we will subsequently calculate the spectral, temperature, and polarization dependencies of optical properties, such as the light absorption coefficient and LCD, driven by two-photon transitions from the light and heavy hole branches to the spin-orbit split subband, it should be noted that in wide-bandgap (narrow-bandgap) semiconductors, such transitions are allowed in the frequency range $\Delta_{SO}\langle 2\hbar\omega\langle E_g\ (E_g, \Delta_{SO}\langle 2\hbar\omega)$.

Linear-circular dichroism in two-photon transitions from the heavy and light hole branches to the spin-orbit split subband

Next, we will calculate the spectral and polarization dependencies of the LCD coefficient, determined by the probability of two-photon transitions, taking into account the phenomenon of coherent saturation [28, 29]:

$$W^{(2)} = \frac{2\pi}{\hbar}\frac{2\hbar\omega}{I}\left(\frac{eA_0}{m_0c}\right)^2\left\langle\sum_{\vec{k}}\left|\sum_{m,m'=\pm 1/2;\vec{k}}M_{SO,m';lh,m}^{(2)}(\vec{k})\right|^2\left[1+\sum_{\vec{k}}\frac{\alpha_\omega}{(\hbar\omega)^2}\left|\sum_{m,m'=\pm 1/2;\vec{k}}M_{SO,m';lh,m}^{(2)}(\vec{k})\right|^2\right]^{-1/2}\right\rangle\times$$
$$\times\left(f_{lh,\vec{k}}-f_{SO,\vec{k}}\right)\delta\left(E_{SO}(\vec{k})-E_{lh}(\vec{k})-2\hbar\omega\right),\quad (8)$$

Where the symbol $\langle\dots\rangle$ denotes averaging over the solid angles of the wave vector of the holes. Then, the square of the modulus of the two-photon matrix element (ME) is determined by the following relation: for optical transitions of type $|lh,\pm 1/2\rangle\xrightarrow{2PA}|SO,\pm 1/2\rangle$.

$$\Re_{SO,lh}^{(1)} = \frac{\frac{1}{2}\left(\frac{eA_0}{c\hbar}\right)^4\left(\frac{B^2k^2}{\hbar\omega}\right)^2\left(\Re_Z e_z'^4+\Re_\perp e_\perp'^4+\Re_{Z\perp}e_\perp'^2 e_z'^2\right)}{\sqrt{1+4\frac{\alpha_\omega}{\hbar^2\omega^2}\frac{1}{2}\left(\frac{eA_0}{c\hbar}\right)^4\left(\frac{B^2k^2}{\hbar\omega}\right)^2\left(\Re_Z e_z'^4+\Re_\perp e_\perp'^4+\Re_{Z\perp}e_\perp'^2 e_z'^2\right)}},\quad (9)$$

for optical transitions of type $|lh,\pm 1/2\rangle\xrightarrow{2PA}|SO,\mp 1/2\rangle$

$$\Re_{SO,lh}^{(2)} = \frac{\left(\frac{eA_0}{c\hbar}\right)^4\left(\frac{B^2k^2}{\hbar\omega}\right)^2\Re_{Z\perp}'e_\perp'^2 e_z'^2}{\sqrt{1+4\frac{\alpha_\omega}{\hbar^2\omega^2}\left(\frac{eA_0}{c\hbar}\right)^4\left(\frac{B^2k^2}{\hbar\omega}\right)^2\Re_{Z\perp}'e_\perp'^2 e_z'^2}},\quad (10)$$

where

$$4\frac{\alpha_\omega}{\hbar^2\omega^2}\frac{1}{2}\left(\frac{eA_0}{c\hbar}\right)^4\left(\frac{B^2k^2}{\hbar\omega}\right)^2 = \xi_R\left(\frac{\Delta_{SO}}{\hbar\omega}\right)^6\left[\frac{\mu_{SO,lh}}{4\mu_{hh,lh}}\left(2\frac{\hbar\omega}{\Delta_{SO}}-1\right)\right]^2,\quad (11)$$

$\xi_R = 2\alpha_\Delta\left(\frac{I}{I_\Delta}\right)^3\frac{e^4}{B^2k_\Delta^2}$ - is the Rabi parameter, $k_\Delta^2 = \frac{2\mu_{hh,lh}}{\hbar^2}\Delta_{SO}$, $\alpha_\Delta = 6\frac{\Delta_{SO}^2}{\hbar^2}T_n^{(1)}T_{n'}^{(1)}$, $I_\Delta = \frac{cn\omega\Delta_{SO}^3}{(2\pi|B|^2 k_\Delta)}$-represent values in units of light intensity that depend on the band parameters of semiconductors, taking into account the energy conservation law describing two-photon transitions between the light and heavy hole subbands of the valence band. Since the value I_Δ depends on the effective mass of the holes in the spin-orbit split subband and its width, it is therefore influenced by the choice of Kane's model (three-band or four-band).

Thus, the coefficient of two-photon LCD light absorption depends not only on the band parameters of the semiconductor but also on the energy $E_c\left(k_{lh,SO}^{(2\omega)}\right) = \frac{m_{SO}m_{lh}}{m_c(m_{SO}-m_{lh})\hbar^2}(2\hbar\omega-\Delta_{SO})+E_g$ of photoexcited electrons in the conduction band, $E_{hh}\left(k_{lh,SO}^{(2\omega)}\right) = \frac{m_{SO}m_{lh}}{m_{hh}(m_{SO}-m_{lh})\hbar^2}(2\hbar\omega-\Delta_{SO})$ of heavy holes, and $E_{SO}\left(k_{lh,SO}^{(2\omega)}\right) = -\frac{m_{lh}}{m_{SO}-m_{lh}}(2\hbar\omega-\Delta_{SO})-\Delta_{SO}$ of holes in the spin-orbit split subband.

If the contribution of the coherent saturation effect is neglected (i.e.,$\xi_R = 0$), then the average value of $\left\langle\sum_{m,m'=\pm 1/2;\vec{k}}\left|M_{SO,m';lh,m}^{(2)}(\vec{k})\right|^2\right\rangle$ is determined as follows: for linear polarization:

$$\left\langle\left|M_{lh,\pm 1/2;SO,\pm 1/2}\right|^2\right\rangle = \frac{1}{2}\left(\frac{eA_0}{c\hbar}\right)^4\left(\frac{B^2k^2}{\hbar\omega}\right)^2\frac{1}{15}(3\Re_Z+8\Re_\perp+2\Re_{Z\perp}),\quad (12)$$

$$\left\langle\left|M_{lh,\pm 1/2;SO,\mp 1/2}\right|^2\right\rangle = \frac{2}{15}\left(\frac{eA_0}{c\hbar}\right)^4\left(\frac{B^2k^2}{\hbar\omega}\right)^2\Re_{Z\perp}';\quad (13)$$

for circular polarization

$$\left\langle\left|M_{lh,\pm 1/2;SO,\pm 1/2}\right|^2\right\rangle = \left(\frac{eA_0}{c\hbar}\right)^4\left(\frac{B^2k^2}{\hbar\omega}\right)^2\frac{1}{2}\frac{1}{15}(2\Re_Z+7\Re_\perp+3\Re_{Z\perp}),\quad (14)$$

$$\left\langle\left|M_{lh,\pm 1/2;SO,\mp 1/2}\right|^2\right\rangle = \frac{1}{10}\left(\frac{eA_0}{c\hbar}\right)^4\left(\frac{B^2k^2}{\hbar\omega}\right)^2\Re_{Z\perp}'.\quad (15)$$

Thus, the dependence of the probabilities of two-photon transitions from the light hole branch to the spin-orbit split subband, $|V, \pm 1/2\rangle \xrightarrow{2PA} |SO, \pm 1/2\rangle$ and $|V, \pm 1/2\rangle \xrightarrow{2PA} |SO, \mp 1/2\rangle$, for linearly polarized light is determined by the following relationships:

$$\left|M_{lh,\pm 1/2;SO,\pm 1/2}\right|^2 = \frac{1}{2}\left(\frac{eA_0}{c\hbar}\right)^4 \left(\frac{B^2 k^2}{\hbar\omega}\right)^2 \left(\Re_z e'^4_z + \Re_\perp e'^4_\perp + \Re_{z\perp} e'^2_\perp e'^2_z\right), \tag{16}$$

$$\left|M_{lh,\pm 1/2;SO,\mp 1/2}\right|^2 = \left(\frac{eA_0}{c\hbar}\right)^4 \left(\frac{B^2 k^2}{\hbar\omega}\right)^2 \Re'_{z\perp} e'^2_\perp e'^2_z. \tag{17}$$

Here, for linearly polarized light

$$|e'_z|^2 = \frac{1}{2} sin^2 \phi', \left|e'_\pm\right|^2 = 1 - |e'_z|^2 \mp P_{circ} cos \phi' = \frac{1}{2}(1 + co s^2 \phi') \mp P_{circ} cos \phi', \tag{18}$$

and for circularly polarized light

$$\left|e'_z\right|^2 = \cos^2 \phi, \left|e'_z\right|^2 = \sin^2 \phi, \left|e'_\pm\right|^2 = \frac{1}{2}(1 + co s^2 \phi') \mp P_{circ} cos \phi', \tag{19}$$

where $\phi(\phi') -$ is the angle between the vectors $\vec{e}(\vec{q})$ and $\vec{k}$, $\vec{e}$- is the light polarization vector, $\vec{k}(\vec{q})$ is the wave vector of the hole (photon), $P_{circ} -$ is the degree of circular polarization.

It should be noted that the polarization (angular) dependence, as well as the dependence on the Rabi factor for both the probability and the LCD coefficient, driven by two-photon optical transitions, are calculated according to relations (17) and (18). Initially, to simplify numerical calculations, we will ignore the contribution of the coherent saturation effect to the transition probabilities.

The spectral and angular dependence of the transition probabilities $|lh, \pm 1/2\rangle \xrightarrow{2PA} |SO, \pm 1/2\rangle$ ($W^{(linear)}_{lh,\pm 1/2;SO,\pm 1/2}$) and $|lh, \pm 1/2\rangle \xrightarrow{2PA} |SO, \mp 1/2\rangle$. ($W^{(linear)}_{lh,\pm 1/2;SO,\mp 1/2}$ for linear polarization in GaAs and InAs semiconductors, calculated according to equations (17) and (18), are shown in Fig. 2. The transition probabilities for $|lh, \pm 1/2\rangle \xrightarrow{2PA} |SO, \pm 1/2\rangle$, and $|lh, \pm 1/2\rangle \xrightarrow{2PA} |SO, \mp 1/2\rangle$ for circular polarization are also depicted in Fig. 2.
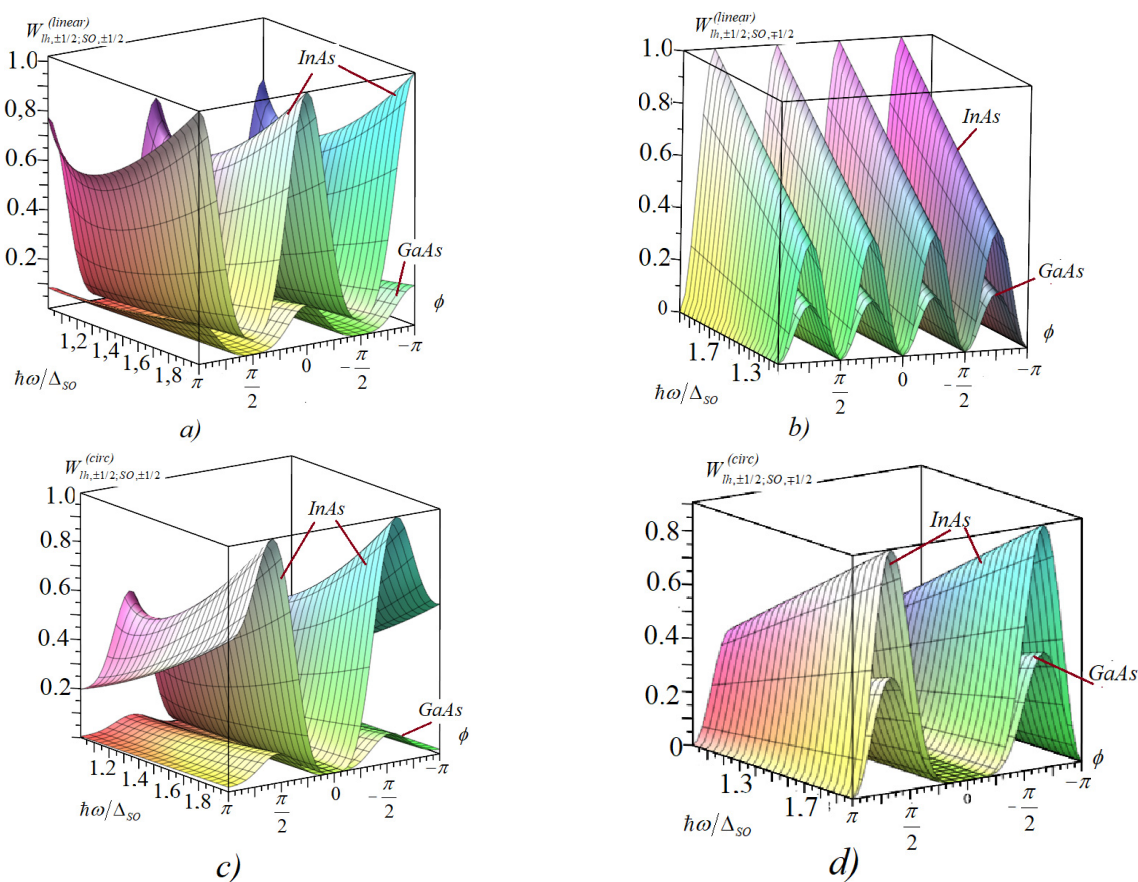

Figure 2. Spectral and angular dependencies of the transition probabilities of type $|lh, \pm 1/2\rangle \xrightarrow{2PA} |SO, \pm 1/2\rangle$ and $|lh, \pm 1/2\rangle \xrightarrow{2PA} |SO, \mp 1/2\rangle$ for linear polarization: (a, c) in *InAs* and (b, d) in *GaAs*

The spectral and angular dependence of the transition probabilities $|lh, \pm 1/2\rangle \xrightarrow{2PA} |SO, \pm 1/2\rangle$, $(W_{lh,\pm 1/2;SO,\pm 1/2}^{(linear)})$, and $|lh, \pm 1/2\rangle \xrightarrow{2PA} |SO, \mp 1/2\rangle$, $(W_{lh,\pm 1/2;SO,\mp 1/2}^{(linear)})$ for linear polarization in GaAs and InAs semiconductors, calculated according to equations (17) and (18), is shown in Fig. 2. For transitions of type $|lh, \pm 1/2\rangle \xrightarrow{2PA} |SO, \pm 1/2\rangle$ and $|lh, \pm 1/2\rangle \xrightarrow{2PA} |SO, \mp 1/2\rangle$ for circular polarization, the results are also presented in Fig. 2.

From Fig. 2, it can be seen that: a) The maximum values of the transition probabilities in InAs semiconductors are significantly higher than those in GaAs, while the oscillation of the angular dependence in InAs and GaAs is identical, i.e., the maximum and minimum oscillation values occur at the same angle in both materials. b) With increasing frequency, the maximum values of $W_{lh,\pm 1/2;SO,\pm 1/2}^{(linear)}$ and $W_{lh,\pm 1/2;SO,\pm 1/2}^{(circ)}$ decrease, passing through a minimum before increasing again, while $W_{lh,\pm 1/2;SO,\mp 1/2}^{(linear)}$ and $W_{lh,\pm 1/2;SO,\mp 1/2}^{(circ)}$ increase in both *InAs* and *GaAs* for both linear and circular polarization.

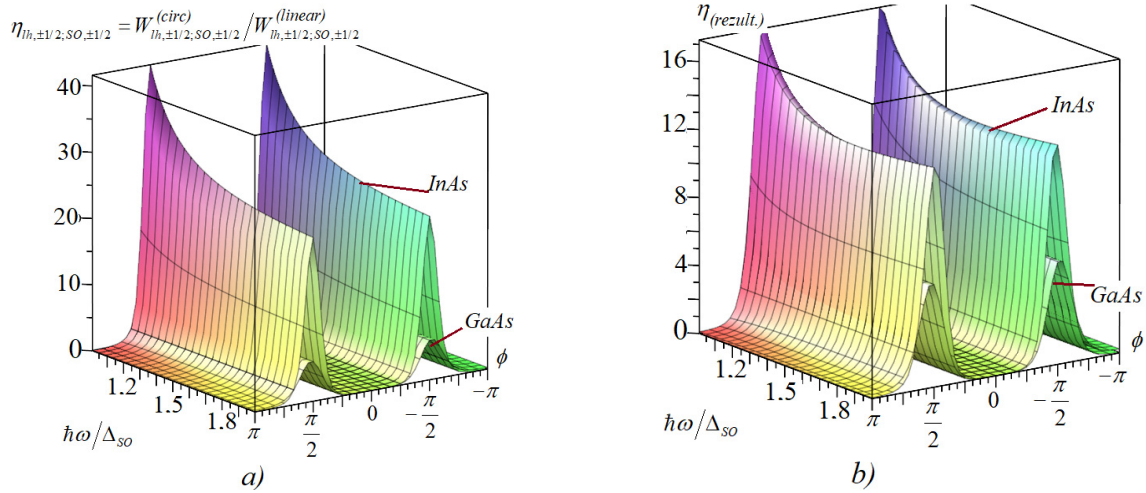**Figure 3.** Spectral and angular dependencies of the two-photon LCD coefficient for optical transitions $\left|lh, \pm \frac{1}{2}\right\rangle \xrightarrow{2PA} \left|SO, \pm \frac{1}{2}\right\rangle$

(*a*) and the resulting LCD (*b*) in *GaAs* and *InAs*, where the contribution of the coherent saturation effect is neglected

Figure 3 shows the spectral and angular dependencies of the two-photon LCD coefficient for optical transitions $|lh, \pm 1/2\rangle \xrightarrow{2PA} |SO, \pm 1/2\rangle$ (Fig. 3a) and the resulting LCD (Fig. 3b) in GaAs and InAs semiconductors. From this figure, it is evident that the two-photon LCD exhibits the following characteristics: In narrow-bandgap semiconductors, it is greater than in wide-bandgap semiconductors. The polarization dependence has an oscillatory nature. With increasing frequency, the maximum value decreases for both semiconductors. It is more significant in the low-frequency region than in the high-frequency region and remains practically unchanged in the frequency range $\hbar\omega \rangle 1{,}5\Delta_{SO}$. Peaks occur at angles $\frac{\pm\pi}{2}$ between the light polarization vector and the wave vector of charge carriers, and these peaks are independent of the type of semiconductor. Now, we proceed to analyze the calculation results considering the contribution of the coherent saturation effect to the probabilities of two-photon transitions. Calculations show that the two-photon LCD coefficient should be distinctly observable in the low-frequency region, as it is proportional to the value $\left(\frac{\Delta_{SO}}{(\hbar\omega)}\right)^6$. Therefore, we will further analyze the contribution of the coherent saturation effect in the frequency range $\frac{\approx\Delta_{SO}}{\hbar}$. First, we calculate the frequency-angular dependencies of the LCD coefficient for several values of the Rabi parameter $\xi_R = 2\alpha_\Delta \left(\frac{I}{I_\Delta}\right)^3 \frac{e^4}{B^2 k_\Delta^2}$: $\xi_R = 0.1$ and $\xi_R = 1.5$

Figure 4 shows the frequency-angular dependencies of the probabilities $W_{lh,\pm 1/2;SO,\pm 1/2}^{(linear)}$ and $W_{lh,\pm 1/2;SO,\mp 1/2}^{(linear)}$ in GaAs and InAs, illuminated by both linearly and circularly polarized light for $\xi_R = 0.1$ and $\xi_R = 1.5$. It can be observed that the physical nature of the probabilities depends on the degree of light polarization, the types of transitions, and the band structure of the semiconductor: a) At a fixed frequency, the angular dependence $W_{lh,\pm 1/2;SO,\pm 1/2}^{(linear)}$ $\left(W_{lh,\pm 1/2;SO,\pm 1/2}^{(circ)}\right)$ exhibits three (two) peaks for transitions $|lh, \pm 1/2\rangle \xrightarrow{2PA} |SO, \pm 1/2\rangle$, and four peaks for transitions $|lh, \pm 1/2\rangle \xrightarrow{2PA} |SO, \mp 1/2\rangle$.

From the latest results (see, for example, Fig. 4a, c, b, d), it is evident that the spectral dependence of the $\eta_{lh,SO} = \frac{W_{lh;SO}^{(sirc)}}{W_{lh;SO}^{(chiz)}}$-two-photon LCD coefficient can only be calculated at certain angle values, since the probabilities of optical transitions for both linearly and circularly polarized light become zero at specific points.
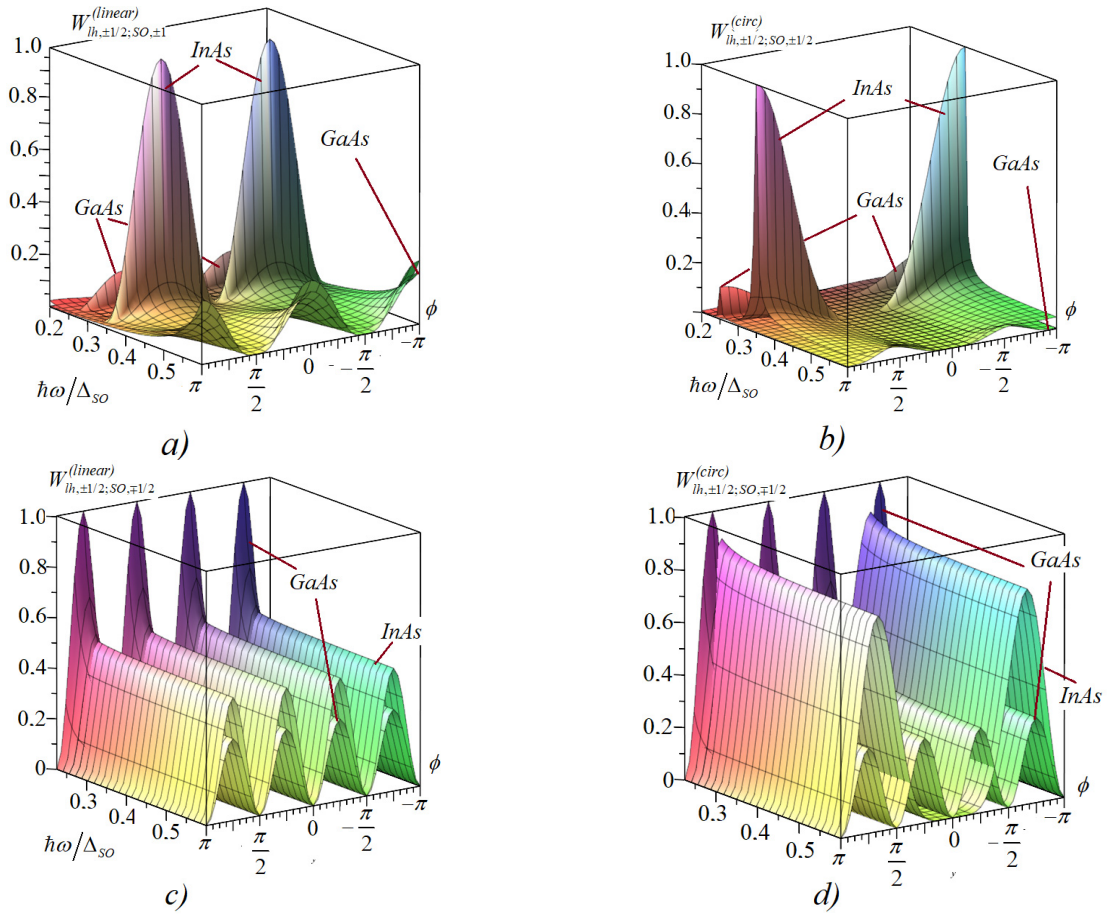
Figure 4. Spectral and angular dependencies of the transition probabilities of type $|lh, \pm 1/2\rangle \xrightarrow{2PA} |SO, \pm 1/2\rangle$ and $|lh, \pm 1/2\rangle \xrightarrow{2PA} |SO, \mp 1/2\rangle$ for linear (a, c) and circular (b, d) polarization in InAs and GaAs. The Rabi parameter is assumed to be 0.1

In such cases, the LCD coefficient remains undefined. Therefore, we will analyze the frequency-angular dependencies of $\eta_{lh, \pm 1/2; SO, \pm 1/2}$ in GaAs and InAs for two angle values between the light polarization vector and the photon wave vector: $\frac{\pi}{6}$ (a) and $\frac{\pi}{3}$ (b) (Fig. 5).
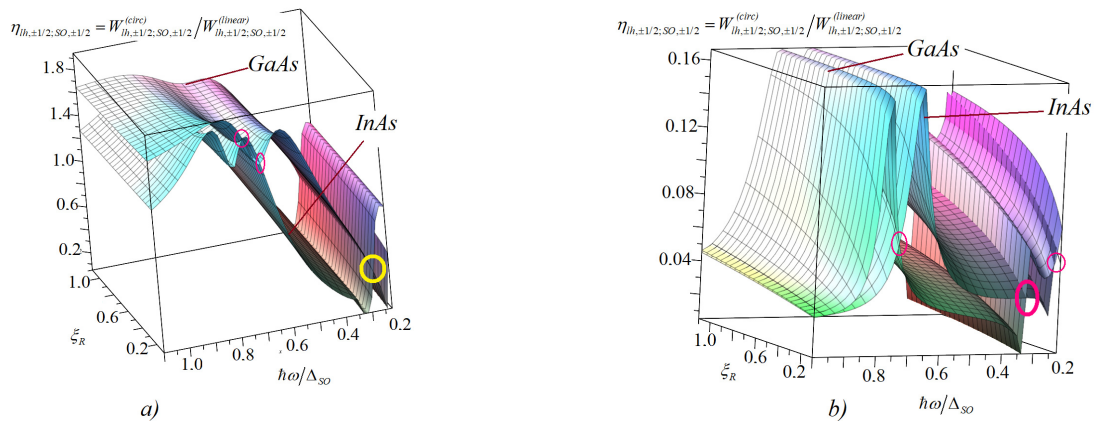

Figure 5. Frequency dependence and dependence on the Rabi parameter of the two-photon LCD coefficient for the angle between the light polarization vector and the photon wave vector equal to $\frac{\pi}{6}$ (a) and $\frac{\pi}{3}$ (b), calculated for optical transitions $|lh, \pm 1/2\rangle \xrightarrow{2PA} |SO, \pm 1/2\rangle$ in GaAs and InAs, where the intersections of the graphs are marked with circles

From Fig. 5, it is evident that the nature of the frequency dependence of the LCD coefficient: a) Depends on the band structure of the semiconductor; b) The amplitude value of $\eta_{lh, \pm 1/2; SO, \pm 1/2}$ is almost ten times greater than that of $\eta_{lh, \pm 1/2; SO, \mp 1/2}$ in both the high- and low-frequency regions for GaAs and InAs.

Fig. 6. Angular dependence and dependence on the Rabi parameter of the resulting two-photon LCD coefficient $\left(\eta_{rezult} = \eta_{lh, \pm 1/2; SO, \pm 1/2} + \eta_{lh, \pm 1/2; SO, \mp 1/2}\right)$ in GaAs and InAs for two frequency values: $\hbar\omega = 0.25 eV$ (a) and $\hbar\omega =$

0.5eV (b). It can be observed that the LCD is more noticeably observed in GaAs than in InAs, but the maximum LCD values in InAs occur at $\frac{\pm\pi}{2}$, and in GaAs at $\frac{3\pi}{4}$ when $\hbar\omega = 0.25eV$; in GaAs at $\frac{11\pi}{8}$, and in InAs at $\frac{\pm 3\pi}{2}$ when $\hbar\omega = 0.5eV$.
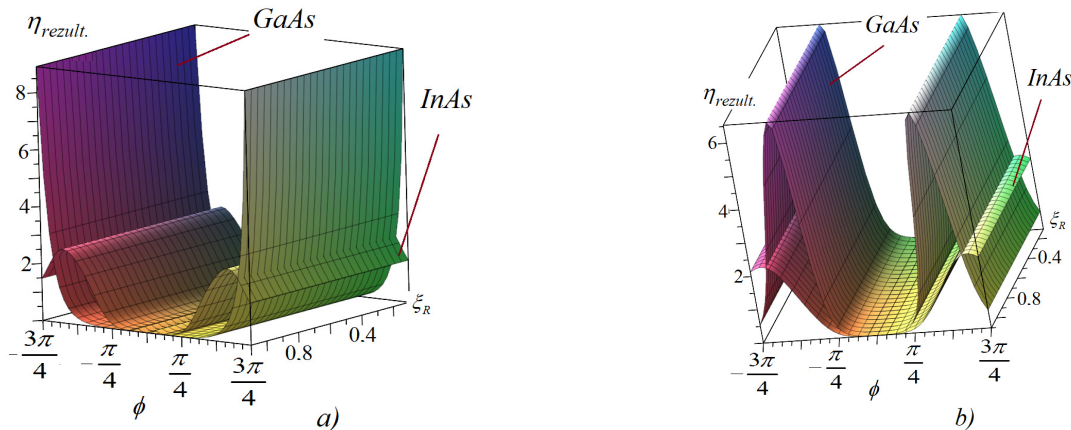

Figure 6. Angular dependence and dependence on the Rabi parameter of the resulting two-photon LCD coefficient $\left(\eta_{rezult} = \eta_{lh,\pm 1/2;SO,\pm 1/2} + \eta_{lh,\pm 1/2;SO,\mp 1/2}\right)$ in GaAs and InAs for two frequency values: $\hbar\omega = 0.25eV$ (a) and $\hbar\omega = 0.5eV$ (b)

Calculations show that if the dependencies $E_g(T)$, $m_c(T)$, $m_{SO}(T)$, calculated using the three-band Kane model, are taken into account, the main contribution to the resulting two-photon LCD coefficient $\langle\eta^{(2)}(\omega,T)\rangle$, averaged over the solid angles of the hole wave vector, comes from transitions of type $|lh,\pm 1/2\rangle \xrightarrow{2 photon absorption} |SO,\pm 1/2\rangle$, while the contribution of transitions $|lh,\pm 1/2\rangle \xrightarrow{2 photon absorption} |SO,\mp 1/2\rangle$ is less than 3%. The calculations also indicate that, without considering the effect of coherent saturation, $\langle\eta^{(2)}(\omega,T)\rangle$ in GaAs and InAs is practically independent of temperature.

Light absorption due to two-photon transitions from the light hole branch of the valence band to the spin-orbit split subband

Thus, the coefficient of two-photon absorption caused by optical transitions between the light hole subband and the spin-orbit split subband is determined by the following relation

$$K^{(2)}(\omega,T) = \frac{2\hbar\omega}{I}\frac{2\pi m_{SO}m_{lh}}{(m_{SO}-m_{lh})\hbar^3}k_{lh,SO}^{(2\omega)}\left[f_{lh}\left(k_{lh,SO}^{(2\omega)}\right) - f_{SO}\left(k_{lh,SO}^{(2\omega)}\right)\right]\times$$

$$\int_0^\pi \sin\theta\cdot d\theta \int_0^{2\pi} d\varphi \left|\sum_{lh,m=\pm 1/2;SO,m'=\pm 1/2} M_{lh,m;SO,m'}^{(2)}\left(k_{lh,hh}^{(2\omega)},\theta,\varphi\right)\right|^2 \tag{20}$$

where $k_{lh,SO}^{(2\omega)}$ is the wave vector of the photoexcited holes, and the matrix element (ME) of the transition $|lh,\pm 1/2\rangle \xrightarrow{2 fotonli yutilish} |SO,\pm 1/2\rangle$ is:

$$M_{lh,\pm 1/2;SO,\pm 1/2} = \left(\frac{eA_0}{c\hbar}\right)^2 \frac{1}{2}\left(\frac{B^2 k^2}{\hbar\omega}\right)^2 \left\{4\left[\frac{A}{B}\frac{\hbar\omega}{E_{SO}-E_{lh}-\hbar\omega} + 4\left(\frac{A}{B}+1\right)\right]\right\}e'^2_z -$$

$$- \frac{P_c^2}{B^2 k^2}\frac{\hbar\omega}{3}\frac{1}{E_{cond}-E_{lh}-\hbar\omega}\left(e'^2_\perp + 4e'^2_z\right) + \frac{3\hbar\omega}{E_{hh}-E_{lh}-\hbar\omega}e'^2_\perp\}, \tag{21}$$

for $|lh,\pm 1/2\rangle \xrightarrow{2PA} |SO,\mp 1/2\rangle$:

$$M_{lh,\pm 1/2;SO,\mp 1/2} = \left(\frac{eA_0}{c\hbar}\right)^2\left[\frac{i}{\sqrt 6}\frac{2(A+B)P_c k}{(\hbar\omega)} + \frac{1}{\sqrt 2}\frac{P_c^2}{(E_{cond}-E_{lh}-\hbar\omega)_z} + \frac{3\sqrt 2 ABk^2}{E_{SO}-E_{lh}-\hbar\omega}\right]e'_-e'_\mp, \tag{22}$$

$f_{lh}\left(k_{lh,SO}^{(2\omega)}\right)\left[f_{SO}\left(k_{lh,SO}^{(2\omega)}\right)\right]$ - are the distribution functions of charge carriers in the light hole subband (spin-orbit split subband), $B^2\left(k_{lh,SO}^{(2\omega)}\right)^2 = \frac{\hbar^2}{2}\left(\frac{m_{hh}-m_{lh}}{m_{lh}m_{hh}}\right)^2\frac{m_{SO}m_{lh}}{(m_{SO}-m_{lh})}(2\hbar\omega - \Delta_{SO})$, $\theta(\varphi)$-are the polar (azimuthal) angles of the hole wave vector. Calculations show that each term in equations (20) and (21) provides comparable contributions to the two-photon matrix element. This indicates that significant contributions are made not only by transitions where the intermediate states are located in the light and heavy hole branches but also in the spin-orbit split subband, as well as in the conduction band.

The average value of the matrix element (ME) (see formula (3.4.2)) is determined as:

$$\left\langle\left|M_{lh,m;SO,m'}^{(2)}\left(k_{lh,SO}^{(2\omega)},\theta,\varphi\right)\right|^2\right\rangle = \int_0^\pi \sin\theta\cdot d\theta \int_0^{2\pi} d\varphi \sum_{lh,m=\pm 1/2;SO,m'=\pm 1/2}\left|M_{lh,m;SO,m'}^{(2)}\left(k_{lh,SO}^{(2\omega)}SO,\theta,\varphi\right)\right|^2.$$

Then: for optical transitions of type: $|lh, \pm 1/2\rangle \xrightarrow{\text{2фотонноепоглощение}} |SO, \pm 1/2\rangle$:

$$\left\langle |M_{lh,\pm 1/2; SO, \pm 1/2}|^2 \right\rangle = \frac{1}{30}\left(\frac{I}{\hbar\omega}\frac{e^2}{c\hbar}\frac{2\pi}{n_\omega}\right)^2 \left(\frac{B^2 k^2}{\hbar}\right)^2 \left(\Re_Z \begin{Bmatrix} 3 \\ 2 \end{Bmatrix} + \Re_\perp \begin{Bmatrix} 8 \\ 7 \end{Bmatrix} + \Re_{Z\perp}\begin{Bmatrix} 2 \\ 3 \end{Bmatrix}\right); \tag{23}$$

and for optical transitions of type: $|lh, \pm 1/2\rangle \xrightarrow{\text{2PA}} |SO, \mp 1/2\rangle$

$$\left\langle |M_{lh,\pm 1/2; SO, \pm 1/2}|^2 \right\rangle = \frac{1}{2}\left(\frac{I}{\hbar\omega}\frac{e^2}{c\hbar}\frac{2\pi}{n_\omega}\right)^2 \left(\frac{B^2 k^2}{\hbar}\right)^2 \frac{1}{15}\left\langle \left(\Re_Z \begin{Bmatrix} 3 \\ 2 \end{Bmatrix} + \Re_\perp \begin{Bmatrix} 8 \\ 7 \end{Bmatrix} + \Re_{Z\perp}\begin{Bmatrix} 2 \\ 3 \end{Bmatrix}\right)\right\rangle. \tag{24}$$

The number indicated at the top (bottom) in expressions (22) and (23) refers to linear (circular) polarization. Thus, if in expression (19) the relations (20)–(23) are taken into account and the effect of coherent saturation is neglected, then:

a) For linearly polarized light:

$$K_{linear}^{(2)} = 2(2\pi)^3 \frac{I}{\hbar\omega}\left(f_{lh,\vec{k}}^{(2)} - f_{SO,\vec{k}}^{(2)}\right)\left(\frac{e^2}{c\hbar n_\omega}\right)^2 \left(\frac{B^2 k^2}{\hbar\omega}\right)^2 \frac{\mu_-^{(SO,lh)}}{\hbar^3} k_{SO,lh}^{(2\omega)} \times$$
$$\times \left\langle \left[3\Re_{z\perp}' + \frac{1}{30}(2\Re_Z + 8\Re_\perp + 3\Re_{Z\perp})\right]\right\rangle; \tag{25}$$

b) For circularly polarized light:

$$K_{circ}^{(2)} = 2(2\pi)^3 \frac{I}{\hbar\omega}\left(f_{lh,\vec{k}}^{(2)} - f_{SO,\vec{k}}^{(2)}\right)\left(\frac{e^2}{c\hbar n_\omega}\right)^2 \left(\frac{B^2 k^2}{\hbar\omega}\right)^2 \frac{\mu_-^{(SO,lh)}}{\hbar^3} k_{SO,lh}^{(2\omega)} \times$$
$$\times \left\langle \left[2\Re_{z\perp}' + \frac{1}{30}(3\Re_Z + 7\Re_\perp + 2\Re_{Z\perp})\right]\right\rangle. \tag{26}$$

The frequency-temperature dependencies of the absorption coefficient $K^{(2)}$, calculated using (24) and (25) for transitions $|lh, \pm 1/2\rangle \xrightarrow{\text{2fotonliyutilish}} |SO, \pm 1/2\rangle$ and $|lh, \pm 1/2\rangle \xrightarrow{\text{2fotonliyutilish}} |SO, \mp 1/2\rangle$ in GaAs (a, c) and InAs (b, d), are shown in Fig. 7. From this figure, it can be observed that: a) In GaAs, the consideration of $E_g(T)$ practically does not affect $K^{(2)}(\omega, T)$, whereas in InAs, it leads to an increase in $K^{(2)}(\omega, T)$. b) The amplitude value of $K_{circ}^{(2)}(\omega, T)$ is greater than the amplitude value of $K_{linear}^{(2)}(\omega, T)$. c) With increasing temperature in InAs, the maximum values of $K_{circ,linear}^{(2)}(\omega, T)$ decrease in the low-frequency region, while in the high-frequency region, they increase instead.
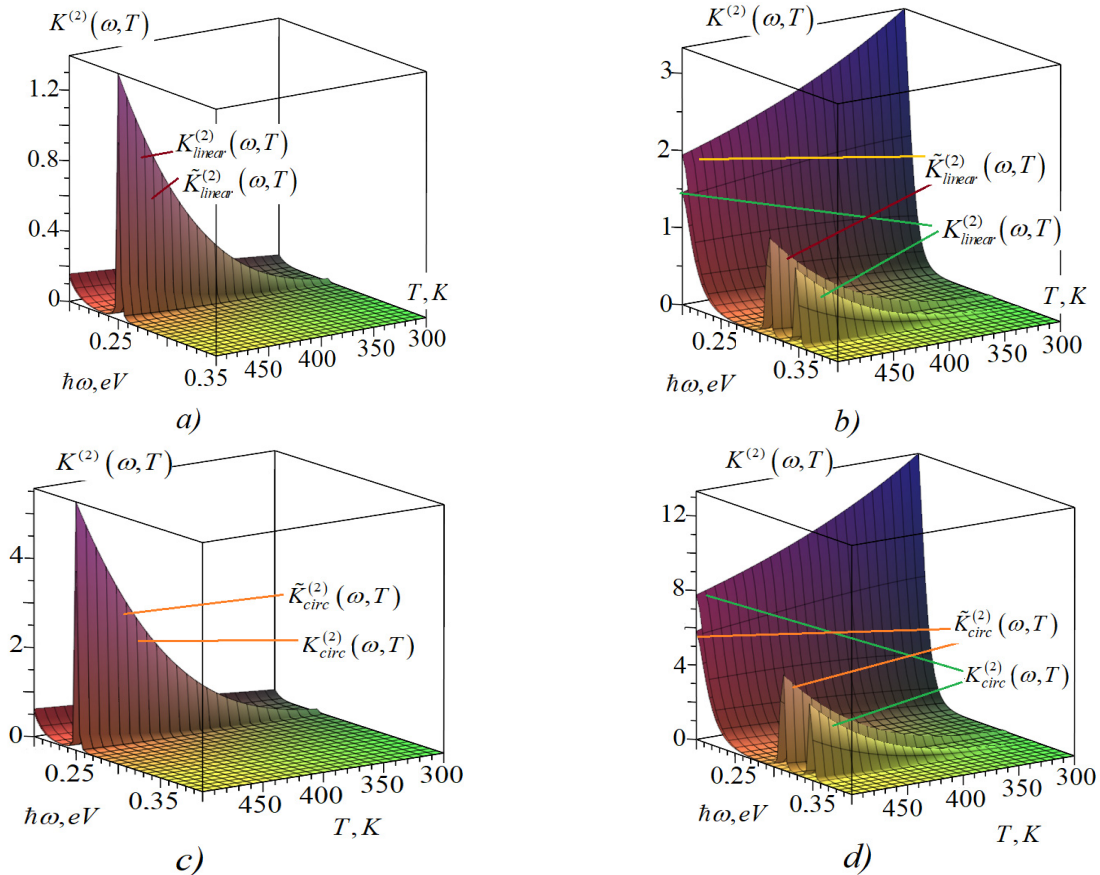

Figure 7. Frequency-temperature dependencies of the two-photon absorption coefficient $K^{(2)}(\omega, T)$ for linearly polarized light (a, b) and circularly polarized light (c, d) in semiconductors GaAs (a, c) and InAs (b, d)

This situation is explained by the ratio of the bandgap width to the spin-orbit splitting width, which is greater than one in GaAs and close to one in InAs.

In the study, the maximum value of $K^{(2)}(\omega, \text{T})$ for linear polarization, calculated for in GaAs, was set equal to one, neglecting the contribution of the coherent saturation effect. $\left(\widetilde{K}^{(2)}(\omega, \text{T})\right)$ represents the 2PA coefficient in cases where the temperature dependence of the band parameters is considered (or not considered).

CONCLUSIONS

Thus, in this work:
1. Based on the multi-band Kane model, interband two-photon absorption (2PA) of light, caused by optical transitions from the light hole branch to the spin-orbit split subband in GaAs and InAs, has been theoretically investigated.
2. Two-photon interband optical transitions have been classified, with attention paid to the fact that virtual states of charge carriers are present not only in the light and heavy hole branches but also in the spin-orbit split subband and the conduction band.
3. In GaAs and InAs, the presence of several peaks in the frequency-temperature dependencies of the 2PA coefficient has been identified. The appearance of the peaks is explained not only by the specific change in the distribution functions of photoexcited holes but also by the fact that, at certain frequency values, some denominators in the expressions for the composite matrix elements tend toward zero.
4. It has been shown that all two-photon optical transitions, which differ by their virtual states, contribute comparably to the absorption.
5. It has been demonstrated that in the frequency regions where the spectral dependence of the probabilities of two-photon transitions changes sharply, two-photon linear-circular dichroism (LCD) can be clearly observed.

ORCID
Rustam Y. Rasulov, https://orcid.org/0000-0002-5512-0654; **Voxob R. Rasulov,** https://orcid.org/0000-0001-5255-5612

REFERENCES
[1] G.I. Stegeman, and R. A. Stegeman, *Nonlinear Optics: Phenomena, Materials and Devices*, (John Wiley & Sons, Inc., Hoboken, NJ, 2012).
[2] E.L. Ivchenko, Sov. Phys. Semicond. **6**, 17 (1973). (in Russian)
[3] V. Nathan, A.H. Guenther, and S.S. Mitra, J. Opt. Soc. Am. B, **2**(2), 294 (1985). https://doi.org/10.1364/JOSAB.2.000294
[4] S.D. Ganichev, E.L. Ivchenko, R.Ya. Rasulov, I.D. Yaroshetskii, and B.Ya. Averbukh, Phys. Solid State, **35**(1), 104 (1993).
[5] I.B. Zotova, and Y.J. Ding, Appl. Opt. **40**, 6654 (2001). https://doi.org/10.1364/AO.40.006654
[6] P.D. Olszak, C.M. Cirloganu, S. Webster, L.A. Padilha, S. Guha, L.P. Gonzalez, S. Krishnamurthy, *et al*., Phys. Rev. B, **82**, 235207 (2010). https://doi.org/10.1103/PhysRevB.82.235207
[7] S.B. Arifzhanov, A.M. Danishevskii, E.L. Ivchenko, S.F. Kochegarov, and V.K. Subashiev. Sov. Phys. JETP, **47**(1), 88 (1978). http://www.jetp.ras.ru/cgi-bin/dn/e_047_01_0088.pdf
[8] R.Y. Rasulov, V.R. Rasulov, M.K. Nasirov, M.A. Mamatova, and I.A. Muminov, East European Journal of Physics, (3), 316 (2024). https://doi.org/10.26565/2312-4334-2024-3-34
[9] V.R. Rasulov, R.Ya. Rasulov, N.U. Kodirov, and U.M. Isomaddinova, Physics of the Solid State, **65**(7), 92 (2023). http://dx.doi.org/10.61011/PSS.2023.07.56410.77
[10] R.Ya. Rasulov, V.R. Rasulov, M.A. Mamatova, M.Kh. Nasirov, and U.M. Isomaddinova, East European Journal of Physics, (3), 310–315 (2024). https://doi.org/10.26565/2312-4334-2024-3-33
[11] V.R. Rasulov, R.Ya. Rasulov, and I. Eshboltaev, Russ. Phys. J. **63**(11), 2025 (2015). https://doi.org/10.1007/s11182-021-02265-x
[12] V.R. Rasulov, R.Ya. Rasulov, I.M. Eshboltaev, and M.X. Qo'chqorov, Semiconductors, **56**(10), 948 (2022). http://dx.doi.org/10.21883/SC.2022.10.55023.9798
[13] D. Yu, Y.Y. Hu, G. Zhang, W. Li, and Y. Jiang, Scientific Reports, **12**(110), 1 (2022). https://doi.org/10.1038/s41598-021-04203-w
[14] H.S. Pattanaik, M. Reichert, J.B. Khurgin, and D.J. Hagan, IEEE Journal of Quantum Electronics, **52**(3), 90000114 (2016). https://doi.org/10.1109/JQE.2016.2526611
[15] E.L. Ivchenko, and G.E. Pikus, *Superlattices and other heterostructures. Symmetry and optical phenomena*, (Springer, Berlin, (1995).
[16] E.L. Ivchenko, *Optical spectroscopy of semiconductor nanostructures*, Alpha Science, (Harrow, UK, 2005).
[17] M.M. Glazov, E.L. Ivchenko, G. Wang, T. Amand, X. Marie, B. Urbaszek, and B.L. Liu, Physica Status Solidi (b), **252**(11), 2349 (2015). https://doi.org/10.1002/pssb.201552211
[18] G. Wang, A. Chernikov, M.M. Glazov, and T.F. Heinz, arXiv:1707.05863v2 (2017). https://doi.org/10.48550/arXiv.1707.05863
[19] S. Shree, I. Paradisanos, X. Marie, C. Robert, and B. Urbaszek, Nature Reviews Physics, **3**(1), 39 (2021). https://doi.org/10.1038/s42254-020-00259-1
[20] R.Ya. Rasulov, V.R. Rasulov, N.U. Kodirov, M.Kh. Nasirov, I.M. Eshboltaev, East European Journal of Physics, (3), 303 (2024). https://doi.org/10.26565/2312-4334-2024-3-32
[21] M. Lafrentz, D. Brunne, B. Kaminski, V.V. Pavlov, A.V. Rodina, R.V. Pisarev, D.R. Yakovlev, *et al*., Phys. Rev. Lett. **110**, 116402 (2013). https://doi.org/10.1103/PhysRevLett.110.116402
[22] M.V. Durnev, and M.M. Glazov, Physics-Uspekhi, **188**(9), 913 (2018). https://doi.org/10.3367/UFNe.2017.07.038172
[23] L.E. Golub, E.L. Ivchenko, and R.Ya. Rasulov, Physics and Technics of Semiconductors, **29**(6), 1093 (1995). (in Russian)
[24] R.Ya. Rasulov, V.R. Rasulov, K.K. Urinova, M.A. Mamatova, and B.B. Akhmedov, East Eur. J. Phys. (1), 393 (2024). https://doi.org/10.26565/2312-4334-2024-1-40
[25] U. Isomaddinova, PhD Thesis, Namangan, Republik of Uzbekistan, (2024). (in Russian)

[26] V.R. Rasulov, R.Y. Rasulov, R.R. Sultonov, and B.B. Akhmedov, "Two- and Three-Photon Linear-Circular Dichroism in Cubic-Symmetry Semiconductors," Semiconductors, **54**(11), 1381–1387 (2020). https://doi.org/10.1134/S1063782620110226

[27] V.R. Rasulov, R.Ya. Rasulov, I.M. Eshboltaev, and M.K. Nasirov, Russian Physics Journal, **58**(12), 1681–1686 (2015). https://doi.org/10.1007/s11182-016-0702-2

[28] N.V. Leppenen, E.L. Ivchenko, and L.E. Golub, Phys. Rev. B, **105**, 115306 (2022). https://doi.org/10.1103/PhysRevB.105.115306

[29] D.A. Parshin, and A.R. Shabaev, ZhETF, **92**(4), 471 (1987). (in Russian)

ДО ТЕОРІЇ ДВОФОТОННОГО МІЖПІДЗОННОГО ПОГЛИНАННЯ ТА ЛІНІЙНО-ЦИРКУЛЯРНОГО ДИХРОЇЗМУ В НАПІВПРОВІДНИКАХ ТИПУ A₃B₅

Рустам Я. Расулов[a], Воксоб Р. Расулов[a], Фаррух У. Касимов[b], Мардонбек Х. Насіров[a,c], Іслам Е. Фарманов[a], Абай З. Турсінбаєв[d]

[a]*Ферганський державний університет, Фергана, Узбекистан*
[b]*Андижанський державний університет, Андижан, Узбекистан*
[c]*Ферганський державний технічний університет, Фергана, Узбекистан*
[d]*Південно-Казахстанський університет Муктара Ауезова, Шимкент, Казахстан*

У статті досліджуються частотно-температурні залежності ймовірності двофотонного поглинання *(2PA)*, зумовленого переходами з гілки легких дірок до підзони спін-орбітального розщеплення, а також лінійно-циркулярного дихроїзму *(LCD)*, пов'язаного з *2PA*, та коефіцієнта двофотонного поглинання світла в напівпровідниках *GaAs* та *InAs*. Розглянуто вплив ефекту когерентного насичення на поглинання. Проаналізовано роль різних типів переходів, які відрізняються віртуальними станами та беруть участь у 2PA. У *GaAs* та *InAs* виявлено наявність кількох піків у частотно-температурній залежності коефіцієнта *2PA*; поява цих піків пояснюється не лише специфічною зміною функцій розподілу фотоактивованих дірок, а й тим, що при певних значеннях частоти деякі знаменники у виразах для складених матричних елементів прямують до нуля.

Ключові слова: *двофотонні оптичні переходи; віртуальні стани; багатофотонні оптичні переходи; коефіцієнт двофотонного поглинання; ефект когерентного насичення; напівпровідник*